Polymer xxx (2011) 1–7

Contents lists available at ScienceDirect

Polymer

journal homepage: www.elsevier.com/locate/polymer

Fracture and fatigue response of a self-healing epoxy adhesive

Henghua Jin [a,c,1], Gina M. Miller [a,1], Nancy R. Sottos [b,c], Scott R. White [a,c,*]

[a] Aerospace Engineering, University of Illinois at Urbana-Champaign, USA
[b] Materials Science and Engineering, University of Illinois at Urbana-Champaign, USA
[c] Beckman Institute, University of Illinois at Urbana-Champaign, USA

ARTICLE INFO

Article history:
Received 30 November 2010
Accepted 5 February 2011
Available online xxx

Keywords:
Self-healing
Adhesives
Epoxy

ABSTRACT

A self-healing epoxy adhesive for bonding steel substrates is demonstrated using encapsulated dicyclopentadiene (DCPD) monomer and bis(tricyclohexylphosphine)benzylidine ruthenium (IV) dichloride (Grubbs' first generation) catalyst particles dispersed in a thin epoxy matrix. Both quasi-static fracture and fatigue performance are evaluated using the width-tapered-double-cantilever-beam specimen geometry. Recovery of 56% of the original fracture toughness under quasi-static fracture conditions occurs after 24 h healing at room temperature conditions. Complete crack arrest is demonstrated for fatigue test conditions that render neat resin and control samples failed. Inspection of fracture surfaces by electron microscopy reveals evidence of polymerized DCPD after healing. These results are the first mechanical assessment of self-healing for thin (ca. 360 μm) films typical of adhesives applications.

1. Introduction

Inspired by living systems, self-healing polymers are designed to repair damage whenever and wherever it occurs. Several different conceptual approaches to self-healing have been explored over the past several years. In the first, microcapsules containing reactive chemical species are incorporated into the native polymer matrix and upon crack damage release their contents and undergo a healing reaction [1–4]. In the second, a vascular network is embedded and serves as a reservoir for healing agent(s) for sequestration and distribution throughout the polymer matrix [5–7]. The third approach utilizes inherently reversible bonding in the matrix polymer to affect healing via thermally reversible reactions [8–10] or reformation of hydrogen bonds [11].

Although a variety of self-healing polymers have been reported [12], application and performance as adhesives for structural bonding remains unexplored. Thin epoxy structural adhesive films are commonly used in aerospace and automotive industries for bonding metallic and composite substrates. They are also the critical performance factor for composite laminate repairs of aluminum aerospace structures [13]. During the repair process, a composite patch (doubler) is attached to the damaged aluminum skin using an epoxy adhesive film. Failure of the repair is most commonly adhesive debonding and can be difficult to detect using nondestructive techniques. Composite double repair has also been recently adapted to steel structures [14] in which a boron-epoxy composite doubler patch is co-cured with an epoxy based adhesive film to form a bonded repair.

Self-healing of epoxy was initially achieved by incorporating a microencapsulated low molecular weight monomer (dicyclopentadiene, DCPD) and a solid phase chemical catalyst (bis(tricyclohexylphosphine)benzylidine ruthenium (IV) dichloride: Grubbs' first generation catalyst) within an epoxy matrix. Epoxy containing 10 wt.% microcapsules (ca. 200 μm) containing DCPD and 2.5 wt.% Grubbs' catalyst yielded as much as 75% recovery of virgin fracture toughness [1]. By systematically studying size and concentration, healing efficiencies as high as 90% were achieved [2]. Improvements in catalyst protection schemes [15] and morphology [16] led to reductions in catalyst concentration and improvements in the healing kinetics.

Translating these results to adhesives presents a number of unique technical challenges. Adhesives are typically applied as thin films over large planar areas and as such, place geometric constraints on the maximum size of microcapsules that can be used. The presence of a microencapsulated liquid phase healing agent and a solid phase catalyst must not interfere with adhesion of the substrate surface and the native epoxy matrix. Finally, the healing chemistry must provide not only good adhesion to the epoxy matrix, but also to the substrate material(s).

In this paper we demonstrate a self-healing epoxy adhesive suitable for bonding steel substrates. The materials system is

* Corresponding author. Aerospace Engineering, University of Illinois at Urbana-Champaign, 104 S. Wright St., Urbana, IL, USA. Tel.: +1 2173331077.
E-mail address: swhite@illinois.edu (S.R. White).
[1] These authors contributed equally to this work.

0032-3861/$ – see front matter © 2011 Elsevier Ltd. All rights reserved.
doi:10.1016/j.polymer.2011.02.011

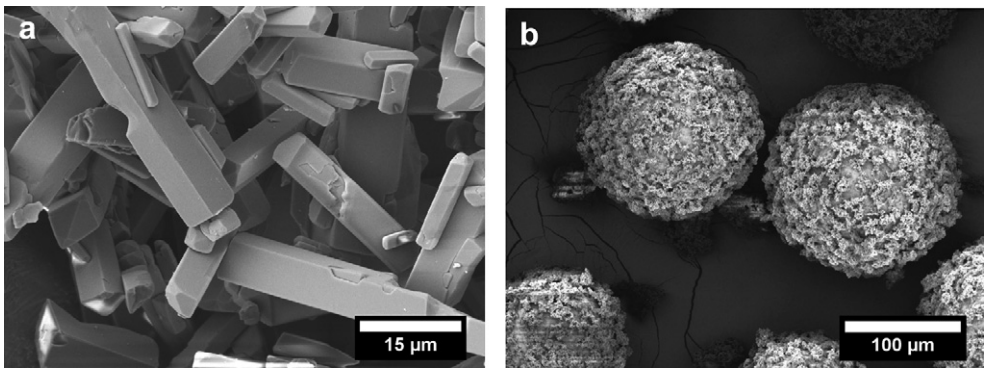

Fig. 1. Scanning electron microscope images of (a) as-received Grubbs' first generation catalyst, (b) DCPD-filled microcapsules with poly(urea-formaldehyde) shell wall.

adapted from our previous studies of bulk epoxy healing consisting of microencapsulated DCPD monomer and Grubbs' first generation catalyst [1]. The quasi-static fracture and fatigue response of adhesively bonded steel samples are presented for a variety of material formulations. Self-healing epoxy adhesives have potential to increase the service life of bonded structures and of laminate repairs for both aerospace and infrastructure applications.

2. Materials

The adhesive matrix consisted of EPON® 828 epoxy resin (DGEBA) (Miller-Stephenson), cured with 12 pph Ancamine® diethylenetriamine (DETA) (Air Products). Both materials were used as-received. The healing chemistry consisted of bis(tricyclohexylphosphine)benzylidine ruthenium (IV) dichloride (Grubbs' first generation) catalyst (Sigma–Aldrich) used as-received (Fig. 1a), and *endo*-dicyclopentadiene (Alfa Aesar), which was distilled prior to encapsulation. Dibutyl phthalate (DBP) (Sigma–Aldrich) was encapsulated as-received and incorporated in control specimens. Silane coupling agent (3-glycidyloxypropyl)trimethoxysilane (Sigma–Aldrich) was used to improve the adhesion between steel substrates and the epoxy adhesive. A 25 μm thick fluoropolymer release film (A4000R) (Airtech International) was molded in specimen to serve as a starter crack. The substrate was A36 structural steel (Speedy Metals).

The DCPD healing agent was stabilized with 150 ppm p-tert-butylcatechol (Acros Organics) and encapsulated following established techniques [17] by *in situ* polymerization of urea-formaldehyde. Microcapsules with average diameter of 130 (±23) μm were produced at 550 RPM agitation rate with a shell wall of

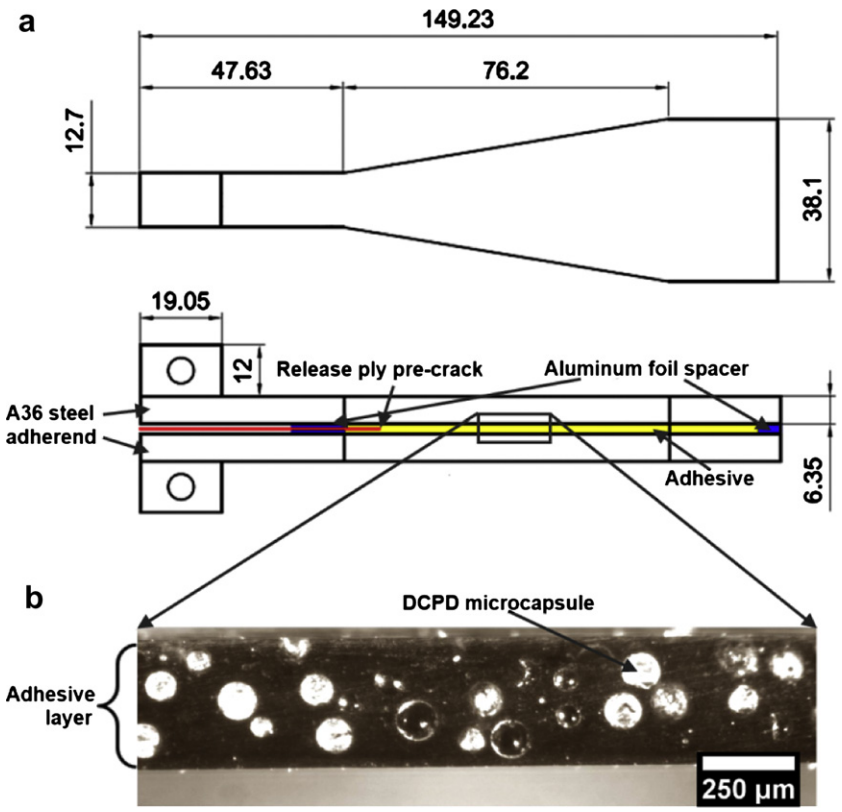

Fig. 2. WTDCB specimen. (a) Geometry of WTDCB specimen consisting of adhesively bonded A36 steel adherends. A 25 μm thick fluoropolymer release ply is used to create a pre-crack. Aluminum foil is used to control adhesive thickness. Dimensions are given in the units of mm. (b) Optical microscopy of cross section of a self-healing adhesive incorporated with Grubbs' catalyst and DCPD microcapsules.

Please cite this article in press as: Jin H, et al., Fracture and fatigue response of a self-healing epoxy adhesive, Polymer (2011), doi:10.1016/j.polymer.2011.02.011

Table 1
Summary specimen types and adhesive components.

Test	Specimen	Adhesive		
		Matrix	Catalyst (wt.%)	Microcapsule (wt.%)
Fracture	Reference control	828/DETA	–	–
	Self-activated control	828/DETA	2.5	–
	Self-healing	828/DETA	2.5	15 (DCPD)
Fatigue	Neat	828/DETA	–	–
	Control	828/DETA	2.5	15 (DBP)
	Self-healing	828/DETA	2.5	15 (DCPD)

approximately 160–220 nm thickness [Fig. 1b]. Mechanical rupture of the shell wall triggers *in situ* polymerization of DCPD by ring-opening-metathesis-polymerization (ROMP) with Grubbs' catalyst producing a tough, highly crosslinked polymer [18]. DBP was encapsulated by the same encapsulation procedure at 550 RPM yielding capsules with average diameter of 122 (±23) μm. Unreactive with Grubbs' catalyst, DBP provided a control case where the effects of the healing reaction were isolated from other material effects.

3. Experimental methods

3.1. Quasi-static fracture testing

The fracture toughness of adhesively bonded steel substrates is measured by preparing and testing width-tapered-double-cantilevered-beam (WTDCB) specimens (Fig. 2a). The WTDCB geometry provides a crack length independent measurement of Mode-I fracture toughness [19–21], critical to accurate analysis of healing performance. Assuming the adhesive layer is thin and does not significantly contribute to the total specimen thickness, linear elastic fracture analysis of the WTDCB geometry yields the mode-I stress intensity factor [22],

$$K_{\mathrm{I}} = 2Pk\sqrt{\frac{3E_a}{(1-\nu^2)E_s h_s^3}} \tag{1}$$

where P is the applied load, k is the taper ratio (for this study, $k = 3$ is used), v_s (0.33) is the adherend (substrate) Poisson's ratio, h_s is the substrate thickness, and E_a (3.4 GPa [23]) and E_s (200 GPa) are the modulus of elasticity of the adhesive and the substrate, respectively. The healing efficiency is defined as the ratio of the healed fracture toughness to the virgin fracture toughness [2]. For the WTDCB geometry the healing efficiency reduces to the ratio of critical fracture loads of the healed and virgin tests,

$$\eta = \frac{K_{\mathrm{IC}}^{\mathrm{healed}}}{K_{\mathrm{IC}}^{\mathrm{virgin}}} = \frac{P_c^{\mathrm{healed}}}{P_c^{\mathrm{virgin}}}. \tag{2}$$

Fracture toughness testing was performed using an Instron 8500 load frame with a 4000 N load cell in displacement control at a rate of 20 mm/min until a crack opening displacement (COD, measured by crosshead extension) of $\delta = 2$ mm was reached. For some control specimens, healing solutions were injected directly into the crack plane while the specimen was held open under load. After the initial (virgin) fracture test, the specimens were unloaded to allow the fracture surfaces to come into contact and heal. After 24 h of healing at room temperature, the specimens were reloaded until a total COD of 2 mm was reached.

3.2. Fatigue testing

The fatigue performance of the self-healing adhesive was also investigated using the WTDCB test geometry. Specimens were tested in the Instron load frame while applying a cyclic stress to propagate the crack. A 2 Hz haversine waveform was applied with a maximum stress intensity of $K_I^{\max} = 0.42$ MPa$\sqrt{m}$ and a stress intensity ratio ($R = K_I^{\min}/K_I^{\max}$) of 0.1. Crack growth was monitored by the measured specimen compliance [22],

$$\Delta a = \sqrt{\frac{CE_s h_s^3}{12k}} - a_0 \tag{3}$$

where $C = \delta/P$ is the compliance of the specimen and a_0 is pre-crack length. Fatigue specimens were fractured after healing and the final crack lengths were measured optically to confirm the calculated final crack length.

3.3. Specimen fabrication

Steel adherends were prepared for bonding by manual sanding using 80 grit sandpaper, cleaning with compressed air and acetone, followed by wiping using acetone to remove debris from the surface. Adherends were then rinsed with a 1 vol.% silane coupling agent solution, dried at room temperature for 30 min, and cured in a 60 °C oven for 1 h. Six layers of 25-μm aluminum foil were then attached to both the beginning of tapered region and the end of the sample (see Fig. 2b) to control the thickness of adhesive layer.

Epoxy adhesive was prepared by mixing EPON 828 with 12 pph DETA curing agent. The epoxy mixture was degassed for 15 min to thoroughly remove entrapped air bubbles before pouring onto each prepared adherend surface. For samples that contained capsules and/or catalyst, these were mixed into the epoxy resin at the appropriate concentration and then degassed for several additional minutes. Thereafter, the mixture was evenly spread across the adherend surfaces and a 25 μm thick fluoropolymer release ply was placed at the beginning of the taper region extending approximately 5 mm along the length of the specimen to serve as a pre-crack. Two adherends were mated together and the specimen was cured at room temperature for 24 h followed by 24 h at 35 °C. After the cure cycle was complete, two loading blocks with through holes for pin loading were attached to the end of each specimen by screws (Fig. 2c).

Three types of specimens were prepared for the quasi-static fracture study (see Table 1). The reference control specimens

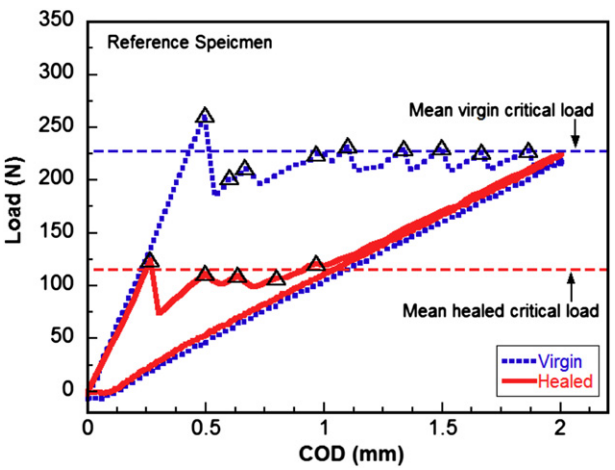

Fig. 3. Representative virgin and healed load versus crack opening displacement (COD) curves for reference specimens. The triangles represent the values used to calculate the mean critical loads of both virgin and healed tests. The upper dash line is the mean virgin critical load (228 N) and the lower dash line is the mean healed critical load (115 N).

Please cite this article in press as: Jin H, et al., Fracture and fatigue response of a self-healing epoxy adhesive, Polymer (2011), doi:10.1016/j.polymer.2011.02.011

Table 2
Summary of quasi-static fracture test results.

Specimen	# of Samples	Fracture Toughness (MPa•m$^{1/2}$)		Healing Efficiency (%)	Adhesive Thickness (μm)
		Virgin	Healed		
Reference	7	0.65 ± 0.04	0.26 ± 0.07	41 ± 11	363 ± 21
Self-activated	8	0.78 ± 0.08	0.33 ± 0.07	44 ± 13	359 ± 23
Self-healing	12	0.82 ± 0.08	0.45 ± 0.19	56 ± 24	375 ± 21

contained only neat EPON 828/DETA epoxy adhesive. Healing for the reference specimen occurs via injection of a pre-catalyzed mixture of 0.5 mL DCPD and 2.5 mg Grubbs' catalyst into the crack plane using a syringe. A second set of controls (self-activated) containing 2.5 wt.% Grubbs' catalyst in the epoxy adhesive were also prepared. These controls provided evidence of catalyst survival and activity in the epoxy matrix. Healing for the self-activated samples was accomplished by injection of 0.5 mL DCPD monomer into the crack plane. Fully *in situ* specimens contained both 2.5 wt.% Grubbs' catalyst and 15 wt.% DCPD-filled microcapsules in the EPON 828/DETA epoxy adhesive (Fig. 2b).

Three types of fatigue specimens were prepared for testing following the same procedures established for fracture toughness samples. In addition to neat epoxy adhesive and fully *in situ* self-healing adhesive, control samples were made incorporating 15 wt.% DBP-filled microcapsules and 2.5 wt.% Grubbs' catalyst in order to isolate the effect of self-healing on the extension of fatigue life (Table 1).

3.4. Fractography

Fracture surface morphology of both quasi-static and fatigue fracture samples were examined using a field emission environmental scanning electron microscope (Philips XL30 ESEM-FEG). Samples were sputter-coated with gold-palladium before imaging.

4. Results and discussion

4.1. Quasi-static fracture

A representative loading curve for a reference specimen is shown in Fig. 3 for the initial (virgin) test and the healed test. In the virgin case load increases linearly with COD until a critical load (~260 N) after which stick-slip, unstable crack propagation occurs at a consistent critical load until reaching a total COD of 2 mm. At this point, a pre-catalyzed mixture of 0.5 mL DCPD monomer and 2.5 mg Grubbs' catalyst is injected into the crack plane, and the specimen unloaded. After 24 h of healing at room temperature, the specimen is retested and follows the virgin loading curve until reaching a healed critical load (~125 N) at which point the crack advances through the healed region. Once the crack fully propagates through the initial fracture region, the loading curve follows the same contour as the virgin unloading path until a total COD of 2 mm is reached. The average virgin and healed critical loads are calculated based on the individual propagation events during the virgin and healed tests, (as indicated in Fig. 3). For this particular specimen, the average virgin and healed critical loads are 228 N and 115 N, respectively. The healing efficiency as defined in Eq. (2) is $\eta = 51\%$. The average healing efficiency for all reference tests is $\eta = 41 \pm 11\%$ and the full results for all quasi-static fracture tests are presented in Table 2.

A representative test result for a self-activated test specimen is presented in Fig. 4. Again, loading is initially linear up to a critical load for crack propagation in both virgin and healed tests. The average virgin and healed critical loads for this specimen are 271 N and 138 N, respectively, yielding a healing efficiency of $\eta = 51\%$. The average healing efficiency over eight tests for self-activated specimens is $\eta = 44 \pm 13\%$ (Table 2). There is a significant increase in virgin toughness for self-activated specimens compared to the neat resin adhesive [23].

Fig. 5 shows typical loading curves for the fully *in situ* self-healing specimen. In this case the virgin loading curve possesses the same characteristic stick-slip propagation mechanism until reaching a COD of 2 mm. However, the healed loading curve is distinctly

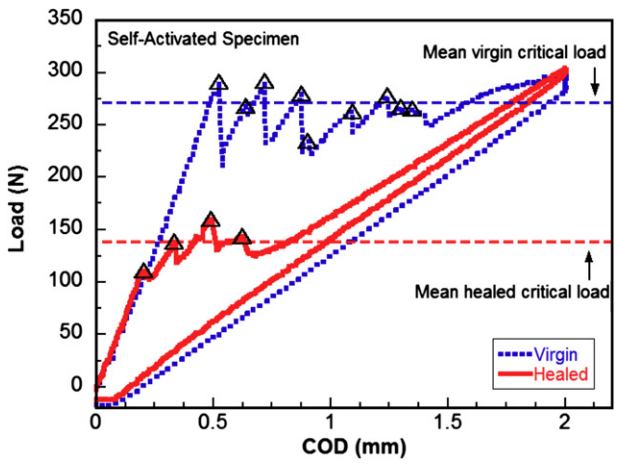

Fig. 4. Representative virgin and healed load versus crack opening displacement (COD) curves for self-activated specimens. The triangles represent the values used for the mean critical loads of both virgin and healed tests. The upper dash line is the mean virgin critical load (271 N) and the lower dash line is the mean healed critical load (138 N).

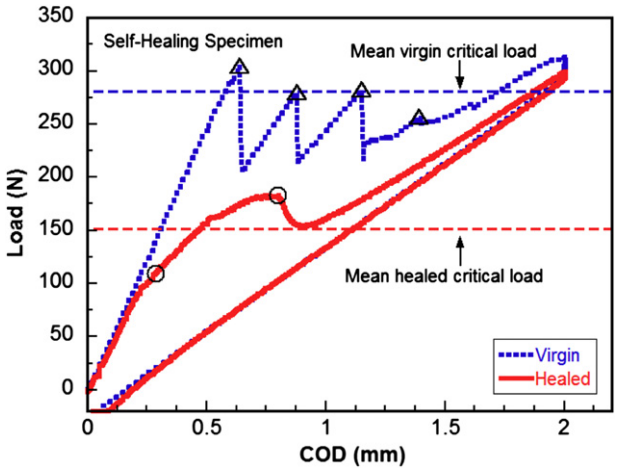

Fig. 5. Representative virgin and healed load versus crack opening displacement (COD) curves for self-healing specimens. The triangles represent the values used for the mean critical load of virgin test. The healed critical load is the mean value of the data between circles. The upper dash line is the mean virgin critical load (281 N) and the lower dash line is the mean healed critical load (151 N).

Please cite this article in press as: Jin H, et al., Fracture and fatigue response of a self-healing epoxy adhesive, Polymer (2011), doi:10.1016/j.polymer.2011.02.011

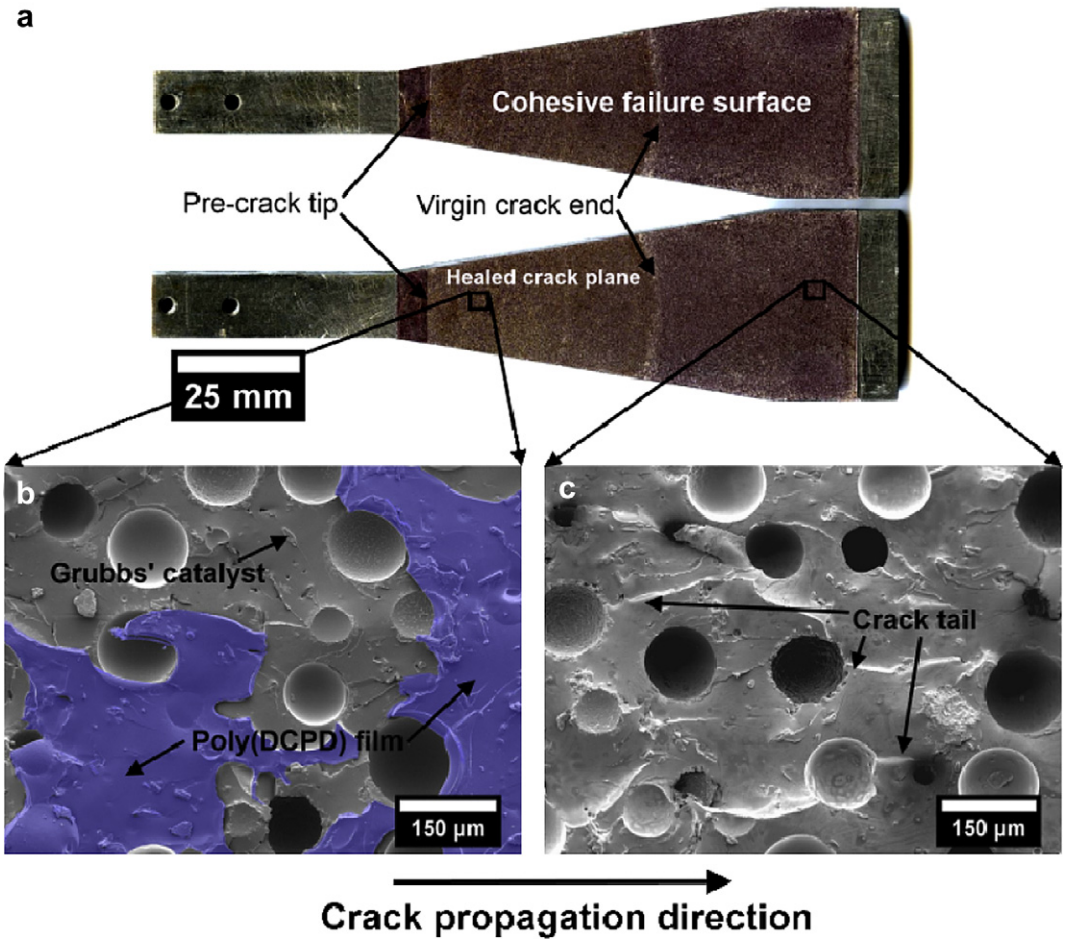

Fig. 6. Quasi-static fracture plane after healing of a self-healing specimen. (a) Optical images of mating fracture surfaces showing cohesive fracture. (b) SEM image of healed fracture surface showing poly(DCPD) film (blue) formed during self-healing. (c) SEM image of fracture surface at the end of the sample created during imaging (unhealed) revealing crack tails indicative of toughening mechanism. (For interpretation of the references to color in this figure legend, the reader is referred to the web version of this article.)

unique from reference and self-activated test cases. After initiating propagation of the healed crack, stable and continuous crack propagation occurs throughout the healed region. This characteristic behavior was observed for all twelve specimens tested. The average virgin critical load (281 N) is obtained by sampling the critical loads associated with the propagation events in the virgin loading trace. For the healed test, we obtain the mean value during crack propagation as designated by the symbols on the loading trace. The initial point is defined based on a 10% deviating in slope from the virgin test and the final point corresponds to the peak load during propagation of the healed crack. Sampling over this COD range yields the average healed critical load of 151 N which corresponds to a healing efficiency of $\eta = 54\%$. The average healing efficiency for all *in situ* samples tested is $\eta = 56 \pm 24\%$ (Table 2). Again, the virgin toughness is significantly improved from the neat resin adhesive case [23].

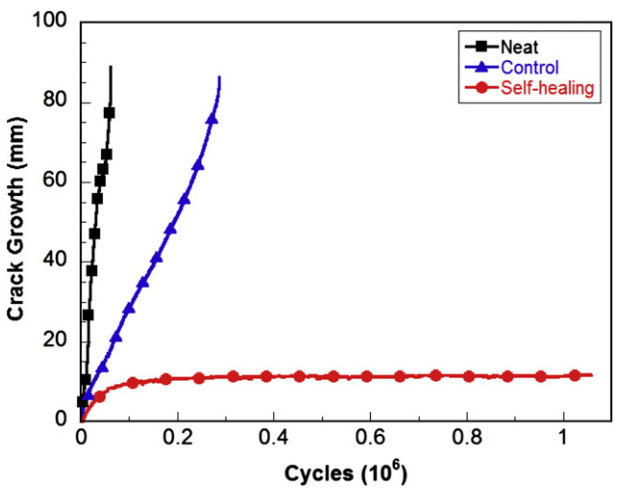

Fig. 7. Representative fatigue response of neat, control and self-healing fatigue specimens. Samples were loaded using 2 Hz haversine waveform at a maximum stress intensity of $K_I^{max} = 0.42$ MPa$\sqrt{m}$ and a stress intensity ratio of $R = 0.1$.

Cohesive failure through the self-healing adhesive was observed for all test cases, an essential requirement for the rupture of embedded microcapsules and activation of the healing mechanism. Surface preparation of the steel adherends by mechanical abrasion, cleaning, and silane coupling agent was applied to promote cohesive

Table 3
Summary of fatigue test results.

Specimen	# of Samples	Crack Growth Rate (μm/cycle)	Cycles to Failure
Neat	4	2.72 ± 1.91	14,940–61,980
Control	4	0.26 ± 0.06	278,220–465,060
Self-healing	4	0[a]	∞[a]

[a] Crack arrest occurs after 150,000 cycles in all cases.

Please cite this article in press as: Jin H, et al., Fracture and fatigue response of a self-healing epoxy adhesive, Polymer (2011), doi:10.1016/j.polymer.2011.02.011

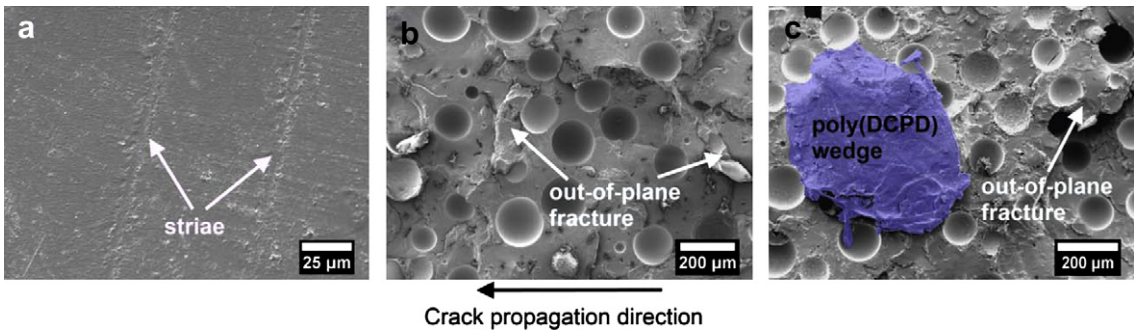

Fig. 8. SEM images of fatigue fracture surfaces for (a) neat, (b) control, and (c) self-healing specimens showing poly(DCPD) wedge (blue). (For interpretation of the references to color in this figure legend, the reader is referred to the web version of this article.)

failure (Fig. 6a). Incorporation of microcapsules and catalyst particles into the adhesive also promotes crack path deflection from the substrate/adhesive interface into the adhesive layer for the self-healing and self-activated control specimens [24–26]. As such, both types of specimens exhibited cohesive failure. However, reference control specimens exhibited a mixture of both cohesive and adhesive failure possibly a result of a change in residual stresses and/or localized T-stress within the epoxy adhesive bondline [27,28].

The improvement in virgin fracture toughness for the adhesive with the addition of self-healing components is consistent with established toughening mechanisms for bulk self-healing polymers [23]. The fracture plane of a virgin test for a self-healing specimen shows extensive crack tail formation characteristic of a crack pinning toughening mechanism (Fig. 6c).

Fractography of healed fracture surfaces reveal the existence of a crosslinked polymer film on the fracture surface (Fig. 6b) indicative of the *in situ* formation of crosslinked poly(DCPD) from the healing reaction. Importantly, this autonomic reaction leads to the recovery of 56% of the virgin fracture toughness on average.

4.2. Fatigue behavior

The representative fatigue response of neat, control and self-healing specimens are shown in Fig. 7. All neat epoxy adhesive specimens failed quickly for the given test conditions (<62,000 cycles), as shown in Table 3. Control specimens containing Grubbs' catalyst and microcapsules containing an unreactive core (DBP) demonstrated significant increase in fatigue life and a reduction in initial crack growth rate (see Table 3). Similar effects have been previously demonstrated in bulk self-healing polymers due to the activation of toughening mechanisms with the addition of microcapsules and as a result of hydrodynamic crack-tip shielding after the release of the encapsulated fluid into the crack plane [29,30].

In stark contrast to both the neat epoxy adhesive and control specimens, full crack arrest occurred for all *in situ* self-healing specimens tested (Fig. 7). After a brief period of initial crack growth (ca. 10 mm) the crack growth rate rapidly decreases until complete arrest occurs. Crack arrest for self-healing specimens occurs largely due to the *in situ* formation of a polymer wedge (as shown in Fig. 8c) in the crack plane preventing full unloading of the crack tip, and a reduction in the effective stress intensity range [29,30]. Additionally, the polymerized healing agent can promote adhesive bonding of the crack faces and a further reduction of the effective stress intensity range. Eventually, the effective stress intensity range is reduced sufficiently and no further crack growth occurs.

Examination of the neat epoxy fatigue specimen by SEM reveals relatively smooth and striated morphology as shown in Fig. 8a. By contrast, the fracture plane for control and self-healing fatigue specimens reveal many out-of-plane fracture features and remnants of microcapsules (Fig. 8b and c). For self-healing specimens, poly (DCPD) wedge features are also present on the fracture plane.

5. Conclusions

A self-healing epoxy adhesive has been demonstrated by incorporating a two-part self-healing system of 15 wt.% microencapsulated dicyclopentadiene (DCPD) monomer and 2.5 wt.% Grubbs' first generation catalyst particles. The addition of both components to the neat resin epoxy increased the virgin fracture toughness by 26% and scanning electron microscopy of fracture surfaces reveals evidence of toughening through crack pinning. Recovery of quasi-static mode-I fracture toughness was assessed using width-tapered-double-cantilever-beam (WTDCB) test specimens. Self-healing specimens recovered 56% of the virgin fracture toughness on average after 24 h healing at room temperature. The fatigue response of self-healing specimens was also investigated at a maximum stress intensity factor of 0.42 MPa•$m^{1/2}$ and a stress intensity ratio of 0.1. The neat epoxy adhesive specimens failed within 62,000 cycles under these conditions while all self-healing samples exhibited complete crack arrest.

Acknowledgments

The authors gratefully acknowledge funding support from National Science Foundation (Grant # CMS 05-27965) and Sandia National Laboratories (SPO 378467) with Dr. Dennis Roach as Program Manager. The authors would also like to thank Kent Elam in the Aerospace Engineering Machine Shop for help manufacturing the WTDCB adherends. Testing was completed at the Advanced Materials Testing and Engineering Lab, with assistance of Peter Kurath, Gavin Horn and Rick Rottet. Electron microscopy was performed in the Imaging Technology Group, Beckman Institute for Advanced Science and Technology at the University of Illinois, with the assistance of Scott Robinson.

References

[1] White SR, Sottos NR, Moore JS, Geubelle PH, Kessler M, Brown E, et al. Nature 2001;409(6822):794–7.
[2] Brown EN, Sottos NR, White SR. Experimental Mechanics 2002;42(4):372–9.
[3] Caruso MM, Blaiszik BJ, White SR, Sottos NR, Moore JS. Advanced Functional Materials 2008;18:1898–904.
[4] Xiao DS, Yuan YC, Rong MZ, Zhang MQ. Polymer 2009;50(13):2697–775.
[5] Williams GJ, Trask RS, Bond IP. Composites A 2007;38(6):1525–32.
[6] Toohey KS, Sottos NR, Lewis JA, Moore JS, White SR. Nature Materials 2007;6:581–5.
[7] Toohey KS, Sottos NR, White SR. Experimental Mechanics 2009;49:707–17.
[8] Chen XX, Dam MA, Ono K, Mal A, Shen HB, Nutt SR, et al. Science 2002;295 (5560):1698–770.
[9] Paisted TA, Nemat-Nasser S. Acta Materialia 2007;55(17):5684–96.

Please cite this article in press as: Jin H, et al., Fracture and fatigue response of a self-healing epoxy adhesive, Polymer (2011), doi:10.1016/j.polymer.2011.02.011

[10] Hayes SA, Zhang W, Branthwaite M, Jones FR. Journal of the Royal Society Interface 2007;4(13):381–7.
[11] Cordier P, Tournilhac F, Soulie-Ziakovic C, Leibler L. Nature 2008;451 (7181):977–80.
[12] Blaiszik BJ, Kramer SLB, Olugebefola SC, Moore JS, Sottos NR, White SR. Annual Review of Materials Research 2010;40:179–211.
[13] Baker AA, Rose LRF, Jones R. Advances in the bonded composite repair of metallic aircraft structure, vol. 1. Elsevier; 2002. pp. 485–516.
[14] Roach D, Rackow K. Sandia report. SAND2005–3195; 2005.
[15] Rule JD, Brown EN, Sottos NR, White SR. Advanced Materials 2005;17 (2):205–8.
[16] Jones AS, Rule JD, Moore JS, Sottos NR, White SR. Journal of the Royal Society Interface 2007;4(13):395–403.
[17] Brown EN, Kessler MR, Sottos NR, White SR. Journal of Microencapsulation 2003;20(6):719–30.
[18] Kessler MR, White SR. Journal of Polymer Science: Part A: Polymer Chemistry 2002;40(14):2373–83.
[19] Kessler MR, Sottos NR, White SR. Composites Part A: Applied Science and Manufacturing 2003;34(8):743–53.
[20] Hwang W, Han KS. Journal of Composite Materials 1989;23(12):396–430.
[21] Jyoti A, Gibson RF, Newza GM. Composite Science and Technology 2005;65 (1):9–18.
[22] Miller G. Self-healing adhesive film for composite laminate repairs on metallic structures, MS thesis. University of Illinois at Urbana Champaign; 2007.
[23] Brown EN, White SR, Sottos NR. Journal of Material Science 2004;39(5): 1703–10.
[24] Grujicic M, Sellappan V, Omar MA, Seyr N, Obieglo A, Erdmann M, et al. Journal of Material Processing Technology 2008;197(1–3):363–73.
[25] Faber KT, Evans AG. Acta Metallurgica 1983;31(4):565–76.
[26] Faber KT, Evans AG. Acta Metallurgica 1983;31(4):577–84.
[27] Fleck NA, Hutchinson JW, Suo Z. International Journal of Solids Structures 1991;27(13):1683–703.
[28] Chen B, Dillard DA. International Journal of Adhesion and Adhesive 2001;21 (5):357–68.
[29] Brown EN, White SR, Sottos NR. Composites Science and Technology 2005;65 (15–16):2466–73.
[30] Brown EN, White SR, Sottos NR. Composites Science and Technology 2005;65 (15–16):2474–80.

Please cite this article in press as: Jin H, et al., Fracture and fatigue response of a self-healing epoxy adhesive, Polymer (2011), doi:10.1016/j.polymer.2011.02.011